Selective catalytic synthesis of 2-ethyl phenol over $Cu_{1-x}Co_x Fe_2O_4$–kinetics, catalysis and XPS aspects

T. Mathew, N.R. Shiju, V.V. Bokade, B.S. Rao, and C.S. Gopinath*

Catalysis Division, National Chemical Laboratory, Dr. Homi Bhabha Road, Pune 411 088, India

Received 12 January 2004; accepted 3 March 2004

A systematic study of catalytic ethylation of phenol is carried out with ethanol as a function of feed composition, time on stream (TOS), temperature, and catalyst composition over $Cu_{1-x}Co_xFe_2O_4$ ($x = 0.0$–1.0) ferrospinel system. Phenol ethylation gives 2-ethyl phenol as a major product under the reaction conditions employed, while its selectivity decreases as temperature and Co-content increases. Compositions containing both Cu and Co ($0 < x < 1$) are found to be more efficient for better catalytic performance than the end compositions ($x = 0$ and 1); $x = 0.5$ shows the highest catalytic performance. TOS studies clearly exhibit the stable activity for $x \leq 0.75$ for at least 50 h. X-ray photoemission spectra (XPS) and X-ray induced Auger electron spectroscopy analysis revealed the partial reduction of metal ions during reaction. Valence band studies clearly show an increase in overlap of metal-ion 3d bands from fresh to spent catalysts by a large decrease in energy gap between them. Cu-rich compositions display a large amount of Cu species on the surface and highlight its importance in the ethylation. High catalytic activity displayed by $0 < x < 1$ emphasizing the importance of both Cu and Co for better catalytic performance.

KEY WORDS: spinel; $Cu_{1-x}Co_xFe_2O_4$; phenol; ethylation; alkylation; 2-ethyl phenol; X-ray photoemission spectra (XPS); X-ray initiated Auger electron spectra (XAES); 3d bands overlap; surface composition.

1. Introduction

Alkyl phenols are industrially important compounds and employed in the manufacture of pharmaceuticals, pesticides, herbicides, plastics, special grade paints and a variety of chemicals [1]. Conventional friedel crafts catalyst for the production of alkyl phenols is uneconomic and acid-waste makes the process non eco-friendly [2]. Solid acid catalysts are very important alternatives to the above and among various solid-acid catalysts, oxides and mixed metal oxides [3–6] are the best for the selective formation of ortho alkyl phenols. 2-ethyl phenol (2EP) resulting from the ethylation of phenol is a valuable chemical and it is used as a starting material for photochemicals [1]. It is also an intermediate for the synthesis of benzofuran, which in turn with indene are the raw materials used for the production of indene-coumarone resins [7]. 2EP and 2,6-diethyl phenol are produced industrially by ortho alkylation of phenol with ethylene in high-pressure autoclaves at 320–340 °C and 20 mPa in the presence of 1–2% aluminum phenolate. Various types of catalysts have been reported to prepare 2EP, including Th/Al oxides, Fe–Si–Mg oxides, phosphoric acid-SiO_2, Fe_2O_3, Cr_2O_3, magnetite, hydrotalcites and Al_2O_3 oxides [1,6,8–11]. However, these catalysts possess one or more of the drawbacks such as, low conversion, severe operative conditions, poor selectivity due to number of side products and lack of reproducibility.

* To whom correspondence should be addressed.
E-mail: gopi@cata.ncl.res.in

Recently Rao and coworkers [12–16] established the idea of using ferrospinel (AB_2O_4, where A = Ni, Co, Cu and Zn and B = Fe) for aromatic C and/or N methylation of compounds like pyridine, aniline and phenol. Low temperature precipitation method is adopted for preparing the ferrospinel catalysts [17]. Diverse properties of the spinel compounds is derived from the possibility of synthesis of multicomponent spinel by partial substitution of cations in position A and B giving rise to $(A_xA'_{1-x})(B_yB'_{2-y})O_4$. Among the spinels, inverse spinels have got special attention due to redox nature of metal ions and the lack of site-specific preference of cations, which enable them to redistribute between octahedral (O_h) and tetrahedral (T_d) sites during the course of catalytic transformation keeping the spinel structure intact. This accounts for the variety of reactions in which they have been used as catalyst.

Recently we have employed ferrospinel based on Cu and Co, namely $Cu_{1-x}Co_xFe_2O_4$, shows an excellent performance towards phenol methylation both in terms of conversion and ortho selectivity [16,18–20] and characterized well for acidity [21]. As a part of continuing study on phenol alkylation, we have carried out phenol ethylation reactions under a wide variety of reaction conditions and X-ray photoemission spectra (XPS) studies over $Cu_{1-x}Co_xFe_2O_4$ system. Special attention has been paid to understand the associated changes in terms of surface composition and change in oxidation states of metal ions by this reaction from fresh to spent catalysts using XPS.

1011-372X/04/0500–0223/0 © 2004 Plenum Publishing Corporation

2. Experimental

The detailed procedure for the preparation by co-precipitation, various characterization and activity measurement of the catalytic ferrospinel materials is described in our earlier publications [12–16,19,20]. X-ray diffraction (XRD) patterns of the catalysts were recorded using CuK_α radiation ($\lambda = 1.5405$ Å) with a Ni filter (Rigaku Geigerflex). XPS and X-ray initiated Auger electron spectra (XAES) were acquired on a VG Microtech Multilab ESCA 3000 spectrometer using a non-monochromatized MgK_α X-ray source ($h\nu =$ 1253.6 eV) on *in situ* scraped fresh catalyst pellets and powder samples of spent catalysts. Base pressure in the analysis chamber was maintained at 3.6×10^{-10} Torr range. Energy resolution of the spectrometer was set at 0.8 eV at a pass energy of 20 eV. More details about the instrument is available in our earlier refs. [22,23]. Spent catalysts analyzed by XRD and XPS are after ethylation at 375 °C for 10 h with 1 : 5 composition of PhOH : EtOH, unless otherwise stated. XPS data presented here is without smoothening or background correction. However, overlapping peaks from spent catalysts were deconvoluted to show the individual components. For the transition metal core levels (Fe 2p and Cu 2p) background correction was carried out with a combination of Shirley and linear methods, since the Shirley background correction alone is not sufficient. A Lorentzian peak shape was assumed for Cu^+ and a combination of Gaussian and Lorentzian for all other states for 2p levels of Cu and Fe. This is mainly due to the sharp peak reported for Cu_2O and broad peaks for di- and tri valent oxides of Cu and Fe [24–26]. Surface compositions were calculated using the standard procedure involving the area of the peak, Scofield photoionization cross section [27] and an experimentally derived response function of the spectrometer to the variation of the photoelectron kinetic energy (KE).

Catalytic performance of the samples towards phenol ethylation reaction were carried out in vapor-phase setup at atmospheric pressure in a vertical, down-flow, fixed-bed reactor. Three grams of fresh catalyst with a particle size up to 20 mesh was charged in the center of the reactor. Catalyst activation was performed by heating the catalyst in dry air at 500 °C for 6 h and then cooled to the reaction temperature. The reactant mixture, consists of phenol and ethanol, was fed by a syringe pump (ISCO, Model 500D) at a weight hourly space velocity of 0.869 h^{-1} for all the measurements reported. The products were collected in a condenser cooled by ice-cold water and the product analysis was performed by GC, GC-MS and GC-IR methods.

3. Results

3.1. Characterization of $Cu_{1-x}Co_xFe_2O_4$

Catalysts were characterized by several techniques and chemical compositions, structural and textural properties of fresh catalysts are already reported in our earlier papers [19,20]. Figure 1 shows XRD patterns of selected compositions of fresh and spent catalysts. All of them show the characteristic reflections of spinel phase. Considerable amount of CuO and Fe_2O_3 phases observed at $x = 0$ disappears by the addition of Co. XRD pattern of spent catalysts shown in figure 1 also displays all reflections and ascertain the integrity of the spinel structure. In the case of $CuFe_2O_4$ the X-ray diffractogram shows no impurities that are observed on the fresh catalyst, however the metallic Cu, Fe and Fe_xC_y phases were observed alongwith major spinel phase peaks. Decreasing Cu-content increases the reducibility of Fe; however, a small amount of Fe^0 is seen at $x = 1$. The above observations demonstrate the reduction conditions simulated during reaction is due to ethanol reforming confirmed from ethanol alone on ferrospinel results typical reformate products. No change in XRD pattern is observed between fresh and spent $CoFe_2O_4$ hints an irreducible and more robust structure. A small increase in lattice parameter a and crystallite size [28] is observed on spent catalysts (table 1).

Table 1
Chemical Analysis, XRD parameters and surface area of $Cu_{1-x}Co_xFe_2O_4$

Catalyst composition (x)	Metal concentration (wt%)[a]			Crystallite size (Å)[b] Fresh (Spent)[c]	Lattice parameter a (Å) Fresh (Spent)[c]	S_{BET} (m^2/g) Fresh
	Co	Cu	Fe			
0.0	–	27.1	46.2	15.25 (22.81)	8.3898 (8.4037)	28.8
0.25	6.1	20.2	46.7	13.85 (17.69)	8.4051 (8.4105)	34.0
0.50	12.4	13.5	47.1	13.17 (17.23)	8.4012 (8.4071)	43.8
0.75	18.6	6.9	47.3	14.77 (19.32)	8.3982 (8.4013)	36.6
1.0	25.1	–	47.6	14.13 (20.47)	8.3997 (8.4028)	36.8

[a]Chemical analysis results obtained from XRF spectroscopy.
[b]Obtained from Scherrer Equation (Ref. 28).
[c]Spent catalysts are after phenol ethylation at 375 °C with 5 : 1 ratio of EtOH : PhOH for 10 h.

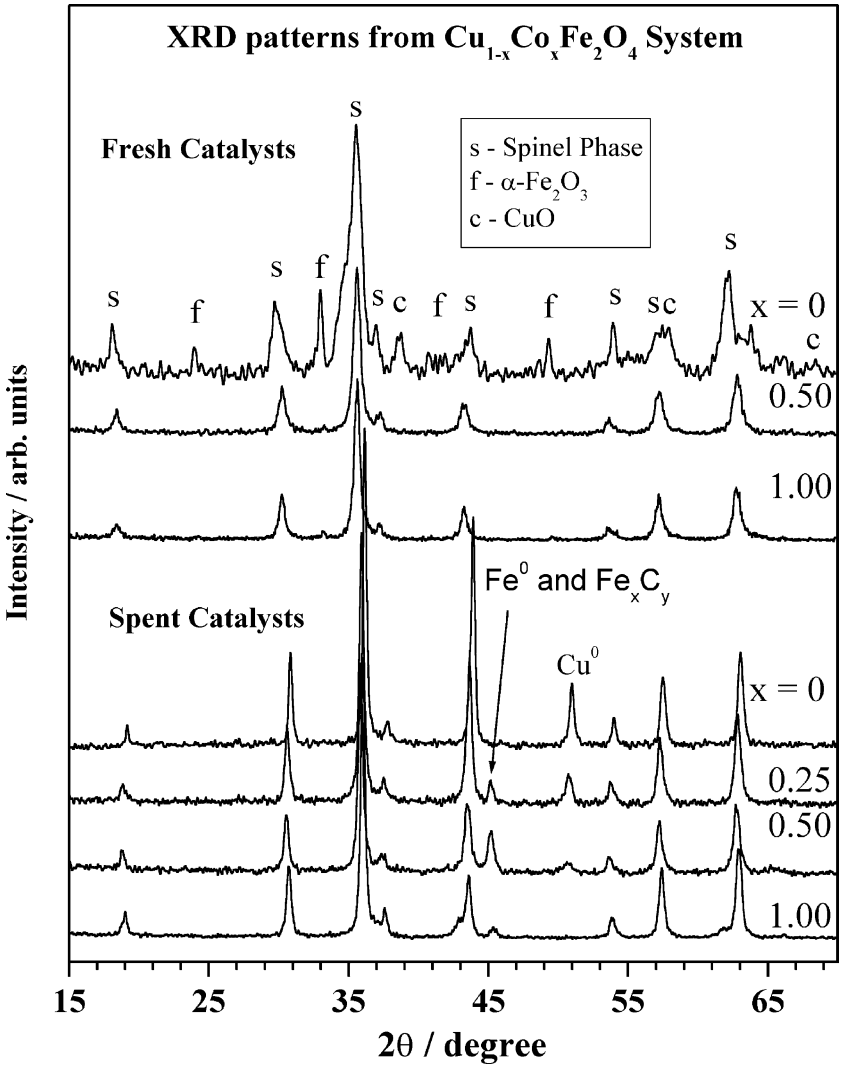

Figure 1. X-ray diffractograms of selected compositions of fresh and spent $Cu_{1-x}Co_xFe_2O_4$ catalysts. XRD from spent catalysts are after phenol ethylation reaction at 375 °C for 10 h with 1 : 5 composition of phenol : methanol. Note an opposite trend in the intensity of metallic Cu and Fe on spent catalysts.

3.2. Catalytic data

Reaction of phenol with ethanol provides ortho ethylated 2EP as major product over $Cu_{1-x}Co_xFe_2O_4$. Side products such as para ethylated phenols, ethyl phenyl ether (phenitole), ethyl methyl phenols, cresols etc. are also formed in very small quantities. Formation of 2,6-diethyl phenol occurs to an extent of 10–15% selectivity at high temperatures.

3.2.1. Effect of ethanol : phenol mole ratio on $Cu_{1-x}Co_xFe_2O_4$

In order to choose an optimum feed mix, phenol ethylation on $x = 0.5$ was carried out at 350 °C using molar ratios of EtOH : PhOH between 3 and 7 (figure 2a). PhOH conversion varies in a volcano shape with increasing EtOH : PhOH ratio with a maximum conversion observed at 5. Hence a mole ratio of 5 : 1 was applied for all results reported in this paper, unless stated. Above trend hints the amount of EtOH is significantly low at a ratio of 3 for a reasonable PhOH conversion. Nevertheless, low conversion at high EtOH : PhOH ratio might be due to excess ethanol in the feed mix causes the decomposition of EtOH as one of the major reaction leaving little room for PhOH ethylation. Test reactions were carried out with EtOH alone on ferrospinels under typical reaction conditions and TGA analysis of spent catalysts demonstrates a coke content equal or higher than that are exposed to 5 : 1 mixture of EtOH : PhOH. Thus, it is evident that ethanol is consumed in other simultaneous reactions, such as ethanol reforming. Formation of reformate products was confirmed by GC and GC-MS analysis. 2EP selectivity remains at a constant high value of 81 ± 2% irrespective of feed ratio at TOS = 3 h. It is to be noted that the catalytic activity expressed in this

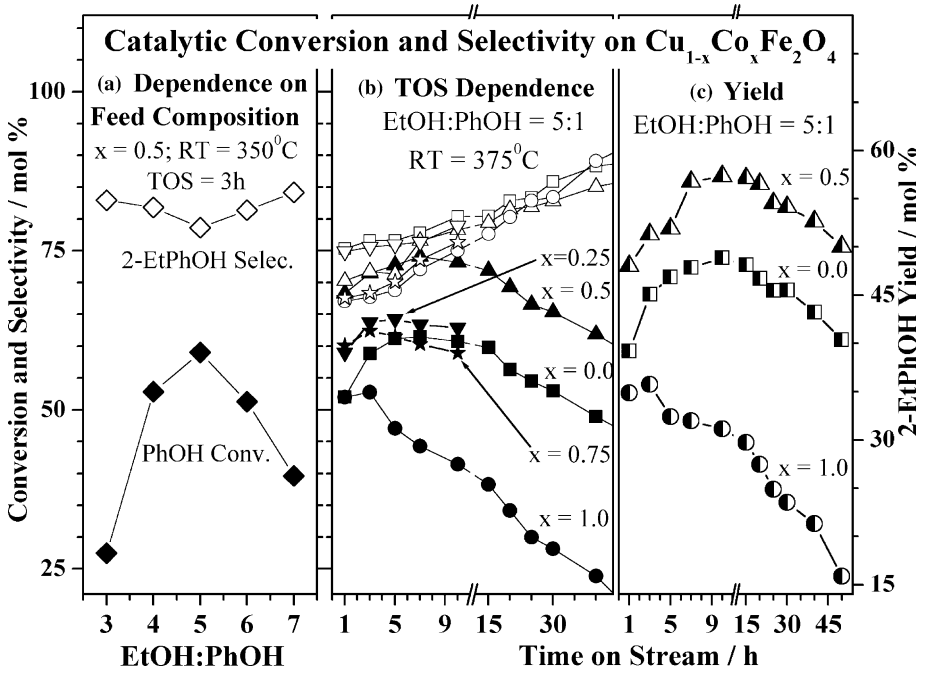

Figure 2. (a) Ethanol : phenol composition dependence of phenol conversion and 2EP (2EtPhOH) selectivity on $Cu_{0.5}Co_{0.5}Fe_2O_4$, TOS = 3 h at 350 °C. (b) Time dependence of phenol conversion and 2EP selectivity at 375 °C; conversion and selectivity is denoted by solid and open symbols, respectively and x values are indicated. Note an increase in product selectivity with increasing TOS and decreasing phenol conversion on Co-rich compositions. (c) TOS dependence of product yield at $x = 0$, 0.5 and 1, shows high and stable yield with Cu-containing compositions.

manuscript is in terms of PhOH conversion and not EtOH conversion, as there are side reactions like reforming, coking due to EtOH on ferrospinels.

3.2.2. Effect of time on stream (TOS)

The stability of the catalysts were studied from the TOS dependence at 375 °C for 50 (10) hours on compositions namely, $x = 0$, 0.5 and 1 (x =0.25 and 0.75) and shown in figure 2b. An increase in PhOH conversion is observed initially up to 5 h for $x \leq 0.75$; almost constant selectivity of 2EP is observed during the above time period with considerable amount of secondary products. Initial TOS up to 5 h is considered to be a transient state (TS). As the time progresses, PhOH conversion and 2EP selectivity reaches apparently to a steady state (SS) with a fluctuation of less than few percent up to 40 h and thereafter deactivation starts very slowly. However, a continuous decrease in activity with increasing TOS is observed on $CoFe_2O_4$. Progressive increase in 2EP selectivity for all x values is due to the retreat of secondary reactions such as formation of aromatics, alkyl phenols etc. observed considerably at low TOS.

A better picture about the TS and SS can be seen in figure 2c with 2EP yield against TOS. Almost an invariable 2EP yield of 47 ± 1% and 56 ± 1% is seen in the SS for $x = 0.0$ and 0.5, respectively. No such SS is seen at $x = 1.0$ indicates the poor activity of $CoFe_2O_4$ towards ethylation. Nonetheless, an equal bulk combination of Cu and Co at $x = 0.5$ displays a high and stable catalytic activity hints the Cu + Co combination is better than $x = 0$ or 1. Further, a product yield at 50 h is comparable or greater than that obtained at 1 h is observed for $x = 0.0$ and 0.5, demonstrates their superior stability. TS and SS observed in the above indicate a considerable modification of the surface from the initial catalyst state to highly reactive state during SS.

3.2.3 Effect of reaction temperature and catalyst composition

The reaction temperature and the catalyst composition dependence of PhOH conversion and 2EP selectivity were investigated and shown in figure 3. Main points are highlighted in the following: (a) All catalyst compositions show an increase in PhOH conversion linearly up to 375 °C and then decreases with further increase in temperature for $0 < x < 1$, but increase marginally for $x = 0$ and 1. However, $x = 0.5$ still shows large PhOH conversion at 400 °C. (b) As the temperature increases the selectivity of 2EP decreases linearly for all compositions, with highest selectivity remains at $x = 0.0$. (c) Positive and negative first order dependence of PhOH conversion and 2EP selectivity, respectively, for all compositions up to 375 °C. (d) At low TOS, high temperature tends to an increase in above mentioned side products, due to which the 2EP selectivity decreases. First two points indicates the influence of Cu + Co combination is a decisive factor from the comparatively large PhOH conversion at $0 < x < 1$ compared to $x = 0$ and 1. Also from the product

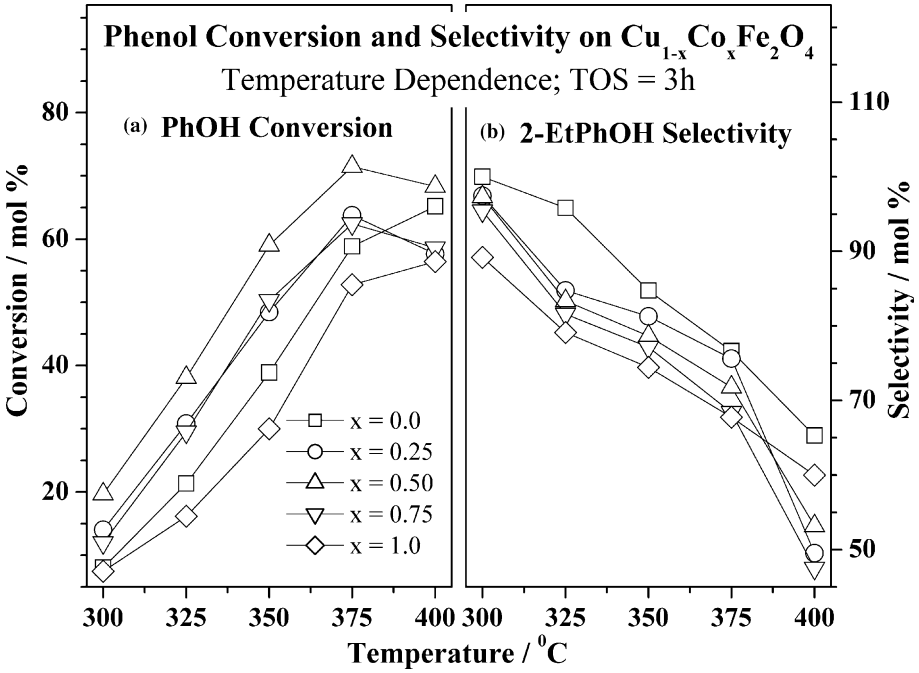

Figure 3. Temperature dependence of (a) phenol conversion and (b) 2EP selectivity is shown for all compositions. Linear increase in phenol conversion and a decrease in 2EP selectivity with increasing temperature indicate the first order dependence of reaction.

analysis, it is found that $0 < x < 1$ produce considerable amount of aromatic hydrocarbons such as benzene and toluene in contrast to end compositions at 400 °C.

3.3. XPS analysis

3.3.1. Cu 2p core level and Cu $L_3M_{45}M_{45}$ Auger transitions

Figure 4 displays the photoemission spectra of Cu $2p_{3/2}$ core level from (a) fresh and (b) spent $Cu_{1-x}Co_xFe_2O_4$ catalysts. It can be noticed that all fresh catalysts (figure 4a) exhibits very similar Cu $2p_{3/2}$ spectra with a main peak at 934.2 ± 0.2 eV and a FWHM of 3.0 eV. Good satellite intensity (I_s) is observed at all x values around 942 eV indicating the existence of Cu^{2+} species. The intensity ratio between the satellite and main line (I_s/I_m) (figure 4c) increases from $x = 0$ to $x = 0.5$ and then decreases at $x = 0.75$. The above variation in I_s/I_m hints that increasing x exerts a marginal and significant influence for $x \leq 0.5$ and 0.75 compositions, respectively, on the population of different final state configurations namely $2p^53d^9$ (satellite) and $2p^53d^{10}L$ (main line), where $2p^5$ and L indicates a hole in Cu 2p level and ligand valence level (O 2p), respectively.

The main features seen from the Cu $2p_{3/2}$ XPS results of spent catalysts (figure 4b) are due to Cu^{2+} species at a BE of 934.2 eV along with the satellites around 942 eV and Cu^+ (and/or Cu^0) at 932.6 ± 0.1 eV. Deconvolution reveals the contribution of the above two Cu-species and Cu-reducibility in terms of lower valent Cu specie to Cu^{2+} is shown in figure 4c along with I_s/I_m. For simplicity, deconvolution is shown only for $x = 0.75$ in figure 4b and the results are given in table 2. Main results from figures 4a–c are highlighted in the following: (1) Cu^{2+} species got partially reduced to Cu^+ (*vide infra*) at all x values during reaction; however, Cu reducibility remains close to 0.44 for $x \leq 0.5$, whereas this ratio is 0.3 at $x = 0.75$. (2) I_s/I_m of $x = 0.75$ increased considerably from fresh to spent, while other compositions does not show a considerable change. Above two points clearly indicates that only at a relatively large Co-concentration ($x = 0.75$), it influences the electronic state of Cu-species significantly.

The Cu $L_3M_{45}M_{45}$ Auger spectra of spent catalysts are shown in figure 4d along with $x = 0.5$ (fresh) catalyst and the modified Auger parameter (α') [24] values calculated are given in table 2. All spent catalysts exhibit a peak centered at 917.2 eV (solid arrow) with a broadening on low KE at 916.2 eV (dotted arrow). Fresh catalyst ($x = 0.5$) contains only Cu^{2+} species, shows the Auger feature only at 917.8 eV. It should be noted here that the KE of Cu $L_3M_{45}M_{45}$ peak for CuO, Cu_2O and Cu occur at 917.6, 916.5 and 918.4 eV respectively; depending on the chemical environment and geometry, the KE of this line has been found to shift significantly [24–26]. The present value for all spent catalysts suggest the contribution of both Cu^+ and Cu^{2+}. No features corresponding to Cu^0 species is seen in the above results indicates the surface metal atoms are oxidized. The bulk metal (Cu) seen in XRD cannot be observed in XPS/XAES due to the above reason of oxidation. In conclusion, there is no significant distortion of Cu^{2+} from fresh to spent catalysts for $x \leq 0.50$

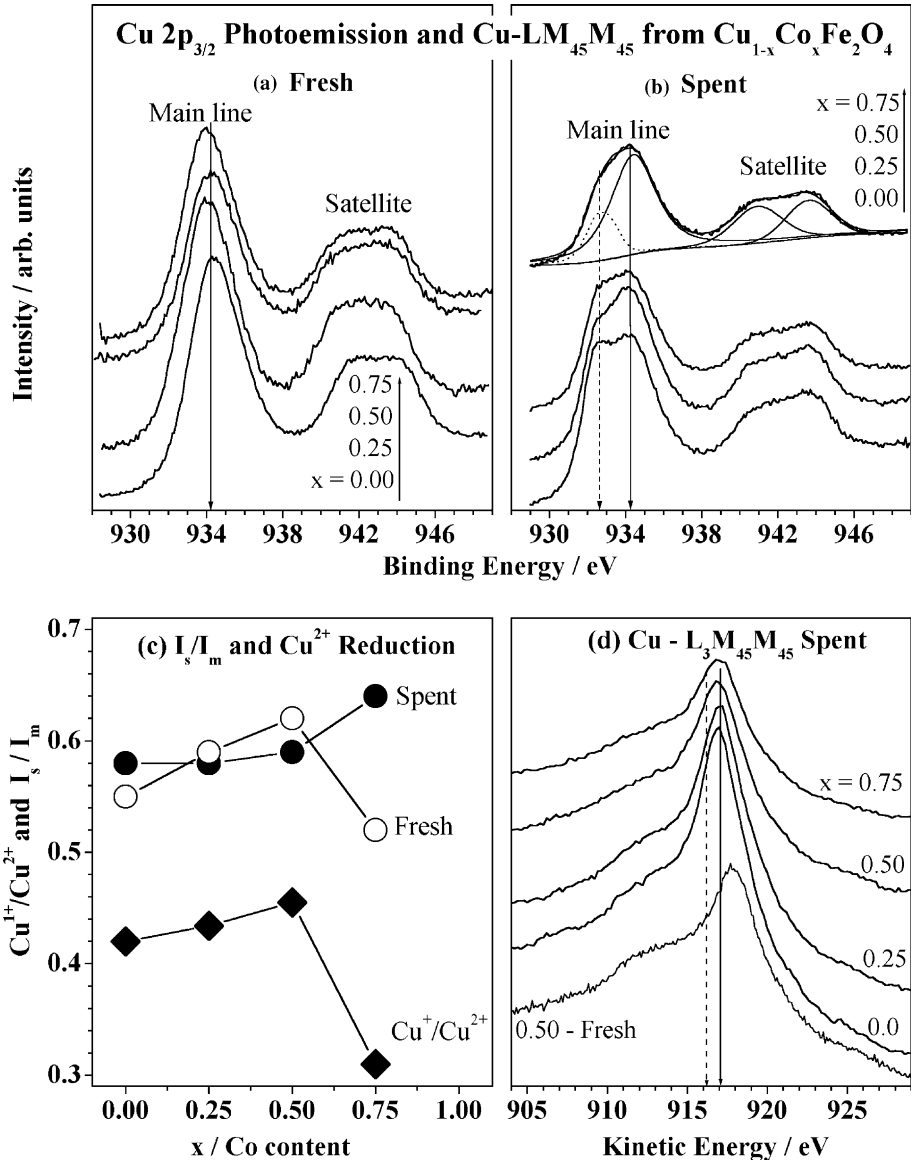

Figure 4. Cu 2p photoemission spectra of (a) fresh and (b) spent $Cu_{1-x}Co_xFe_2O_4$ catalysts. Deconvolution clearly shows both Cu^+ and Cu^{2+} on spent catalysts. Panel c shows the satellite to main line intensity ratio (I_s/I_m) for fresh (F) and spent (S) catalysts and the ratio of reduced Cu to that of Cu^{2+} on spent catalyst. Note a slight increase in the reducibility of Cu from $x = 0$–0.5 and a sudden decrease at $x = 0.75$. (d) Cu $L_3M_{45}M_{45}$ Auger electron spectra of Cu-containing spent catalysts and fresh catalyst ($x = 0.5$ composition) is shown for comparison.

Table 2
XPS and XAES parameters of $Cu_{1-x}Co_xFe_2O_4$ catalysts

Catalyst composition (x)	BE of Cu $2p_{3/2}$ (FWHM) (eV)	KE of Cu $L_3M_{45}M_{45}$ (eV)	α' (eV)
0.00^F	934.3 (3.0)	917.2	1851.5
0.25^F	934.0 (2.9)	917.6	1851.6
0.50^F	934.4 (3.0)	917.8	1852.2
0.75^F	934.0 (3.0)	917.5	1851.5
0.00^S	932.4, 934.1 (4.0)	916.3, 917.0	1848.7, 1851.1
0.25^S	932.6, 934.3 (3.8)	916.2, 917.0	1848.8, 1851.3
0.50^S	932.6, 934.3 (3.9)	916.3, 916.8	1848.9, 1851.1
0.75^S	932.6, 934.4 (3.6)	916.1, 916.9	1848.7, 1851.3

F and S indicate the fresh and spent catalysts.

and the distortion is considerable at $x = 0.75$. High polarizability induced by the formation of Co-containing spinel at high x values would change the nature of Cu–O bonds [29].

3.3.2. Co 2p core level and Co-$L_3M_{45}M_{45}$ Auger transitions

Figure 5 shows Co $2p_{3/2}$ XPS of (a) fresh, (b) spent catalysts and (c) Co-$L_3M_{45}M_{45}$ Auger spectra of $x = 0.5$, 0.75 and 1. XPS derived values of Co 2p levels are given in table 3. The important features observed from Co 2p spectra are: (1) I_s decreases with increasing x. (2) The energy gap between $2p_{3/2}$ peak and its satellite increases with increase in Co-content, especially on spent catalysts (arrow in figure 5b). (3) Energy gap between Co 2p spin orbit doublets (data not shown) increases from fresh to spent catalysts. (4) Two satellite peaks are discernible at $x = 0.75$ and 1; however, only the high BE satellite appears at $x = 1$ on spent catalyst. A comparison of catalysts and various Co-compounds from the literature [20], clearly indicates that the catalysts are in general composed of both Co^{2+} and Co^{3+}. High I_s for $x \leq 0.5$ suggests the contribution of Co^{2+} and high spin Co^{3+}, as low spin Co^{3+} shows poor I_s [30–32]. Figure 5c shows Co-$L_3M_{45}M_{45}$ Auger spectra for $x \geq 0.5$ exhibiting broad features between 760 and 780 eV. Same features at 768 and 772 eV are observed for both fresh and spent catalysts for $x = 1$. However at $x = 0.5$ and 0.75, a shift in energy is seen for lower KE component on spent catalyst compared to fresh. These changes indicate a Cu–Co interaction from near neighbor sites.

3.3.3. Fe 2p core level and Fe – $L_3M_{45}M_{45}$

Figure 6 shows the Fe $2p_{3/2}$ peak and the satellite associated for both (a) fresh and (b) spent $Cu_{1-x}Co_xFe_2O_4$ catalysts. Fresh catalysts exhibit predominant Fe^{3+} peak at a BE of 711 ± 0.2 eV and spent catalysts shows Fe^{2+} and Fe^{3+} [20,33,34]. Important differences between the fresh and spent catalysts are: (a) a reasonable I_S due to predominant Fe^{3+} in O_h coordination

Table 3
XPS parameters from Co 2p core level in $Cu_{1-x}Co_xFe_2O_4$ catalysts

Composition (x)	BE of Co $2p_{3/2}$ mainline (mainline-satellite energy gap) (eV)	$2p_{3/2}$–$2p_{1/2}$ mainline energy gap (eV)
0.5^F	780.5 (4.7)	15.5
0.75^F	780.2 (3.4 and 6.1)	15.6
1.0^F	780.9 (4.6 and 6.1)	15.5
0.5^S	780.7 (3.5 and 5.5)	15.8
0.75^S	780.6 (3.9 and 5.6)	16
1.0^S	780.5 (6.5)	15.9

F and S indicate the fresh and spent catalysts.

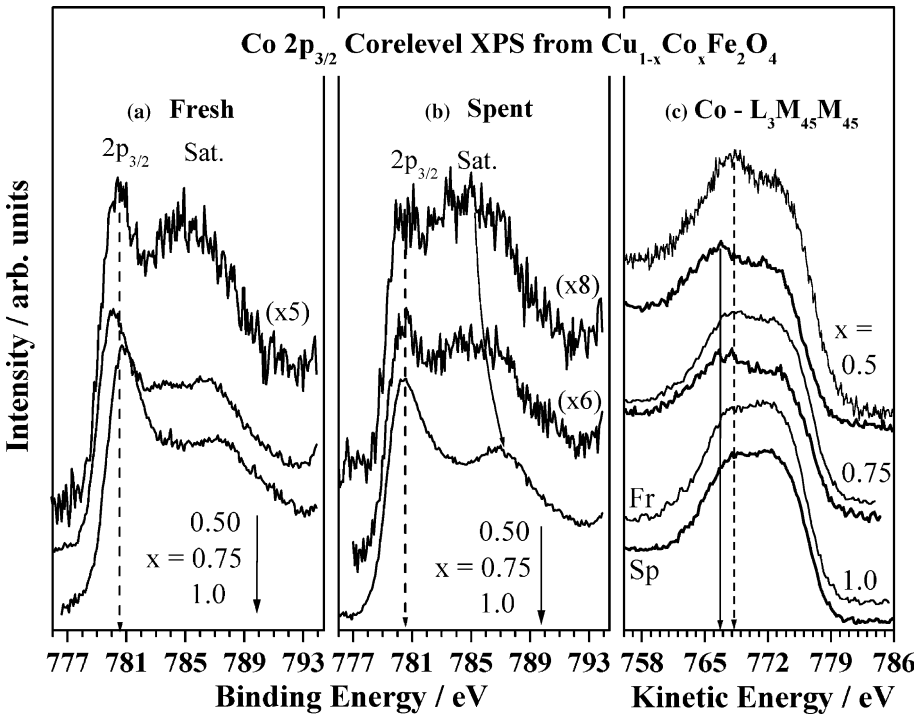

Figure 5. Co 2p core level photoelectron spectra of (a) fresh and (b) spent $Cu_{1-x}Co_xFe_2O_4$ catalysts. Note a decrease in satellite intensity with increasing x on fresh and spent catalysts. (c) XAES from Co $L_3M_{45}M_{45}$ of fresh (thin lines) and spent (bold lines) $Cu_{1-x}Co_xFe_2O_4$ catalysts for $x = 0.5$, 0.75 and 1. Note the changes observed in energy and intensity of $x = 0.5$ and 0.75 from fresh to spent catalysts by dashed and solid arrows, respectively.

[34], is observed on fresh catalysts; (b) partial reduction of Fe is evident on all spent catalysts from the shoulder around 709.6 eV in the main peak and weak I_s, characteristic of Fe^{2+} in T_d coordination [33,34] (broken line in figure 6b) and, (c) a ratio of Fe^{2+} : Fe^{3+} on spent catalysts, (deconvolution shown for $x = 0.5$ in the inset), for all compositions is close to 1 : 1 indicates the partial reduction of Fe. It is to be noted that as such Fe-oxides show low I_s and when the Fe-atoms are in mixed valent state the I_s is further divided and appear at different BE and hence weak I_s [34].

Figure 6c shows the Fe $L_3M_{45}M_{45}$ spectra for representative catalysts ($x = 0.0$ and 0.5). Fe $L_3M_{45}M_{45}$ spectra from fresh catalysts are similar and no difference is observed. However, a shoulder and broadening at low KE is seen for spent catalysts at 696.6 eV (arrow) correspond to Fe^{2+} [20]. Fe 2p and Fe $L_3M_{45}M_{45}$ results indicates the partial reduction of Fe^{3+} to Fe^{2+}.

3.3.4. Valence band studies

Figure 7 shows the VB photoemission spectra of $Cu_{1-x}Co_xFe_2O_4$ for both fresh and spent catalysts. Important changes observed on spent catalysts from core levels are reflected strongly in the VB too. The main VB observed below 10 eV have contributions from metal 3d and O 2p bands and the assignments of various bands are from the photoionization cross section values (σ) at $h\nu = 1253.6$ eV [35] and as explained in our earlier publications [36,37]. Briefly, σ of various bands decreases in the following order Cu 3d > Co 3d > Fe 3d > > O 2p, and indicates large and negligible contribution from Cu 3d and O 2p, respectively to VB. The important observations made from VB region are listed below. (1) Cu and Co 3d bands are separated by more than 2 eV on fresh catalysts; however, on spent catalysts the 3d bands overlap strongly in such a way that the energy gap is less than 1 eV (arrows in figure 7b). (2) Satellite responsible for Cu^{2+} still appears on all Cu-containing spent catalysts with diminished intensity between 10 and 15 eV. (3) Considerable amount of density of states is observed close to 0 eV BE on spent catalysts compared to no intensity on fresh catalysts. (4) A clear shift in Fe 3d bands to lower BE is discernible on all spent catalysts compared to fresh catalysts. (5) Co 3d bands remains at the same BE on fresh and spent catalysts. (6) A general narrowing of metal ion 3d bands on spent catalysts demonstrate a large increase in overlap on spent catalysts compared to fresh catalysts.

3.3.5. Surface composition

Surface composition values for both fresh and spent catalysts from XPS and the PhOH conversion and 2EP yield are given in table 4. This data is helpful to understand the distribution of metal ions and their heterogeneity on the surface, as it directly influences the catalytic activity. The important points worth mentioning are as follows: (1) Cu/Fe, Co/Fe and Cu/Co + Fe ratio changes linearly with x on fresh

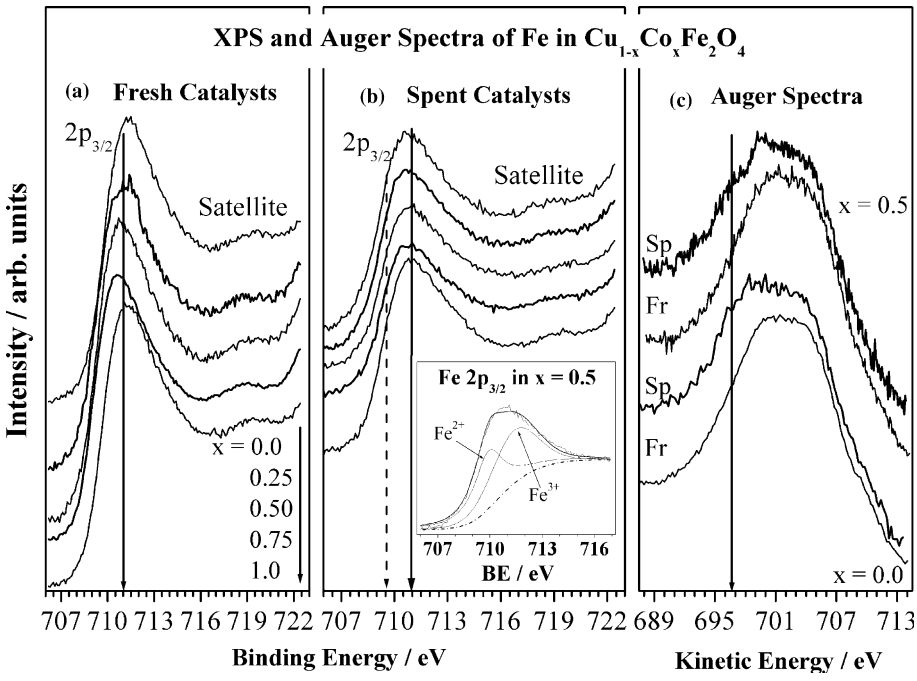

Figure 6. Fe 2p core level XPS of (a) fresh and (b) spent $Cu_{1-x}Co_xFe_2O_4$ catalysts. A shoulder is seen below 710 eV on spent catalysts (dotted line) indicates the partial reduction of iron. Deconvolution of Fe $2p_{3/2}$ peak demonstrate Fe^{2+} and Fe^{3+} on spent catalyst at $x = 0.5$, in the inset on left panel. (c) Auger spectra of fresh and spent $Cu_{1-x}Co_xFe_2O_4$ catalysts.

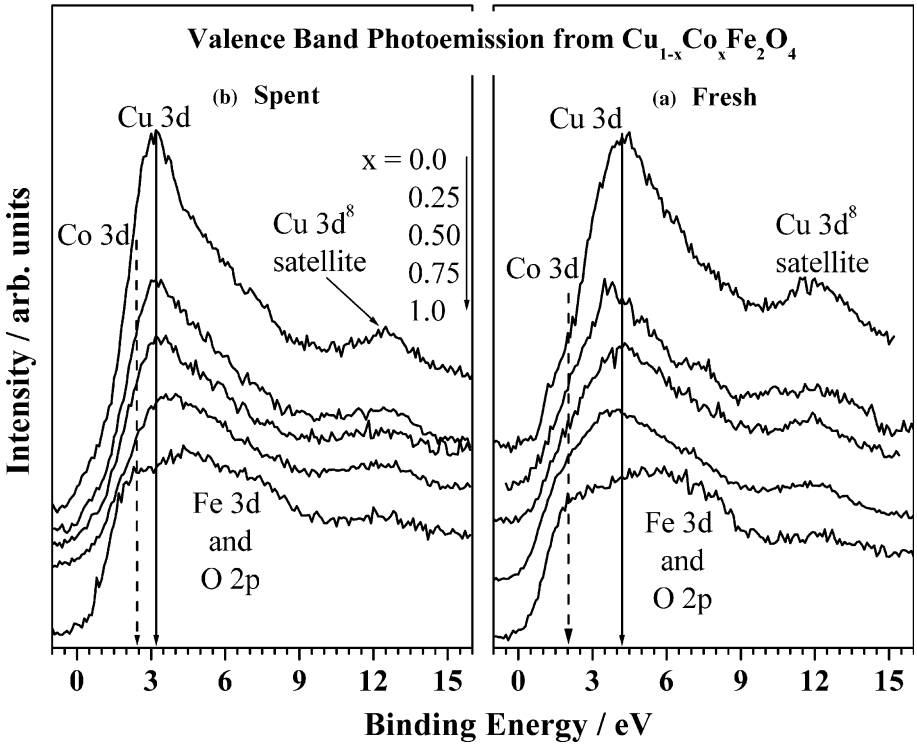

Figure 7. Valence band XPS of (a) fresh and (b) spent $Cu_{1-x}Co_xFe_2O_4$ catalysts. A significant decrease in energy gap between the 3d levels of Cu and Co and a decrease in overall band width is observed on spent catalysts.

Table 4
Surface atomic ratio of fresh and spent $Cu_{1-2}Co_xFe_{2}o_4$ catalysts and the phenol conversion and EtPhoh yeild at TOS = 10^{-h} and $RT = 375$ °C

x	Fresh			Spent						PhOH conversion (mol%)	EtPhOH yield (mol%)
	Cu/Fe	Co/Fe	Co/Co + Fe	Cu/Fe	Co/Fe	Cu/Co + Fe (Cu + Co/Fe)	Fe/C	Cu/C	Co/C		
0.00	1.17	–	1.17	1.26	–	1.26 (1.26)	0.35	0.44	–	60.8	48.9
0.25	1.04	0.20	0.86	1.45	0.18	1.23 (1.63)	0.36	0.53	0.065	62.9	49.7
0.50	0.79	0.32	0.60	1.45	0.30	1.12 (1.75)	0.21	0.31	0.063	73.2	57.4
0.75	0.50	0.50	0.33	1.42	0.33	1.07 (1.75)	0.13	0.19	0.044	58.9	45.0
1.00	–	0.75	0.75[a]	–	1.05	1.05[a] (1.05)	0.46	–	0.49	41.5	31.1

[a]Indicates Co/Fe atomic ratio.

catalysts; however, the surfaces are generally dominated by Cu^{2+} considering the bulk Cu-content, (2) high Cu/Fe and Cu/Co + Fe ratios were found on spent catalysts in comparison with fresh catalysts, in spite of increasing Co-content; however, Co-content on the spent catalysts surface do not vary proportionately with bulk concentration for $x < 1$, (3) significant amount of coke deposition is evident on all compositions, however, it is substantially high at $x = 0.75$, (4) nearly the same Cu/Fe ratio (1.45) is found at $0 > x < 1$ indicates the surface dominance by Cu on spent catalysts too, and (5) heterogeneity of the surface due to distribution of cations is high at $x = 0.5$ and 0.75, indicates that same cations may not be seen in the immediate vicinity and hence large interaction between different metal ions.

Figure 8 displays Cu/Fe and Co/Fe ratio calculated from XPS results in left panel and PhOH conversion with 2EP yield in right panel (table 4), for all catalysts. It is very clear that the ratio of Cu + Co/Fe dominates the catalytic activity rather than a single metal ion content and it is evident from the good correlation of above atomic ratio with reactivity at $0 > x < 1$. Better activity at $x = 0.5$ hints the importance of 1 : 1 bulk ratio of Cu : Co. A heterogeneous distribution of reactive Cu species with Co and Fe is seen at $0 < x < 1$. Cu dominated the surface at $x = 0$ insists the necessity of Co on the surface to achieve better activity. Low PhOH conversion at $x = 1$ hints the poor catalytic activity due to Co + Fe combination. Though $x = 0.5$ and 0.75 shows the same value for Cu + Co/Fe, it is the high coke content decreases the overall activity of $x = 0.75$.

4. Discussion

4.1. Catalytic performance

From the catalytic activity data, it is clear that $0 < x < 1$ compositions are found to have better performance than $x = 0$ and 1 and $x = 0.5$ shows large activity. The selectivity of 2EP decreases with decreasing bulk Cu-content and increasing temperature. This is due to the formation of various C-alkylated products and aromatics. However, an increase in 2EP selectivity is observed as TOS increases (figure 2b) is due to a simultaneous decrease of above side reactions. An almost stable yield observed during SS is due to an increasing 2EP selectivity and a marginal decrease in PhOH conversion. The PhOH conversion shows a volcano type performance with x at all temperatures and a maximum conversion always at $x = 0.5$. Above points hints the ethylation activity is mainly due to Cu + Co combination and among them Cu is highly active towards ethylation.

It is important to mention the key points of FT-IR studies carried out on $Cu_{1-x}Co_xFe_2O_4$ [21] to understand the ethylation activity further. $Cu_{1-x}Co_xFe_2O_4$ surface is dominated by Lewis acid character. A relatively weak acidic character at $x = 0$ increases with Co-content to highly acidic at $x = 1.0$ with an increase in number and strength of acidic sites. A simple correlation of activity and acidity demonstrates that a weak to intermediate acidity favors the reaction.

TOS studies at $x = 0$ and 1 in Figure 2b clearly illustrates the importance of Cu in ethylation. Same initial activity is observed for both $x = 0$ and 1. A continuously decreasing activity with $x = 1$ with TOS is in stark contrast with high and stable activity at $x = 0$. However, a high 2EP selectivity with $x = 1$ indicates that phenol conversion is a limiting factor. A careful look at the surface atomic ratio of $x = 1$ in table 4 indicates the initial Fe-rich surface converted to Fe : Co ratio of 1 : 1 after reaction at 375 °C for 10 h. This indicates the large surface segregation of Co leads to lower activity. Replacement of 50% Co ($x = 0.5$) by Cu leads to an enhanced and stable ethylation activity ascertain that it is the combination of Cu + Co that works better than any single metal–ion enriched surfaces. The above results are in good agreement with FT-IR studies [21] that highly acidic $CoFe_2O_4$ does not favor the ethylation compared to weakly acidic $CuFe_2O_4$. Further spent $CoFe_2O_4$ surface enriched with Co indicates even higher acidity and hence lower activity compared to fresh surface, in agreement with activity and XPS results.

Formation of small amount of phenitole (< 5%) suggests the ethylation might be partly due to isomerization. To clarify the above point, phenitole was reacted with the $x = 0.5$ catalyst at 375 °C. No isomerized products indicate the ethylation is thro direct C-alkylation of PhOH.

The kinetic parameters were evaluated from the PhOH conversion data in the temperature range between 300 and 375 °C in an Arrhenius fashion to highlight the nature of ethylation reaction. Experimental results showed that PhOH ethylation over $Cu_{1-x}Co_x$

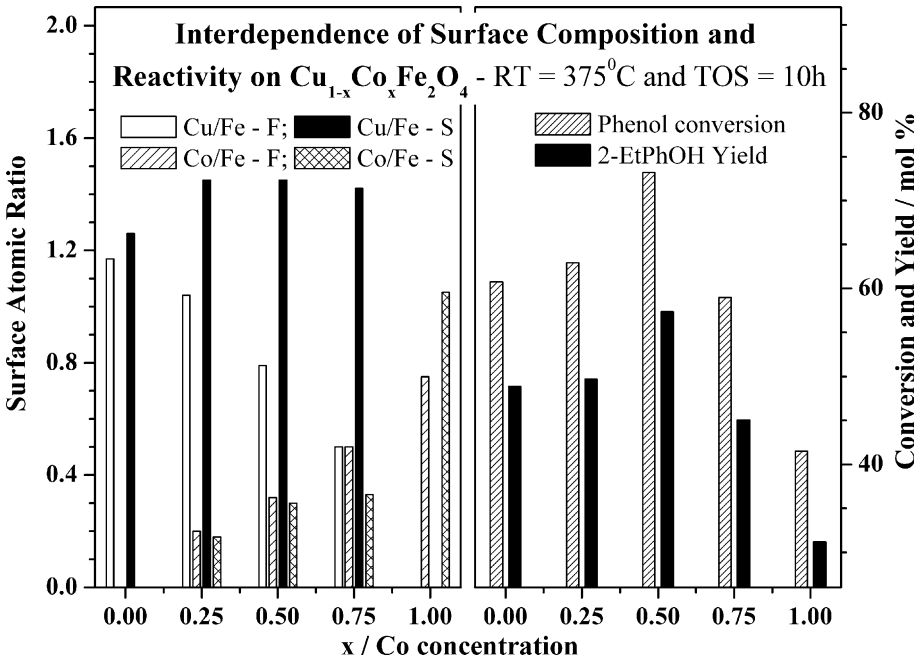

Figure 8. (a) Comparison of phenol conversion and 2-EtPhOH selectivity of $Cu_{1-x}Co_xFe_2O_4$ catalysts at 375 °C, TOS = 10 h and (b) atomic ratio of Cu/Fe and Co/Fe for all fresh (F) and spent (S) catalyst compositions. Note the influence of Co-content and product yield, which is high at $x = 0.5$.

Fe_2O_4 follows first order kinetics with respect to PhOH conversion and hence the rate is assumed to be first order Arrhenius equation. Composition dependent E_a is shown in figure 9. From the kinetic parameters it is clear that $0 < x < 1$ compositions exhibit relatively low E_a towards PhOH conversion than $x = 0$ and 1. The E_a values for the PhOH methylation have been reported in the range of 20–130 KJ/mol over MnO [38], anions loaded $AlPO_4$-Al_2O_3 [39], HZSM-5 [40] and Mg-Al hydrotalcites [41]. The E_a evaluated in the present study varies almost in a close range (94–113 KJ/mol) supports the validity of the model.

It has been shown by several authors that a good correlation exists between E_a and ln A_0 for different reactions taking place over one catalyst [42–45]. Such a correlation is termed as "compensation effect" or "isokinetic effect" and can be written as:

$$E_a = a + b \bullet \ln A \quad \text{(or)} \quad \Delta H = c + d \bullet \Delta S \qquad (1)$$

where a, b, c and d are constants called correlation parameters [44]. The ΔH and ΔS are free energy of enthalpy and entropy. These parameters related to isokinetic temperature (parameter d) and the isokinetic rate constant (parameters a and c). All experimental values (ln A and E_a) within each group of related reactions were included in the linear regression analysis, and the compensation line was calculated using these formulas. Compensation effect on $Cu_{1-x}Co_xFe_2O_4$ can be explained by considering a range of acid sites with different acid strength present [21], and each one of them needing a different E_a for carrying out the reaction. In principle, it can be expected that increase in acidity decrease the increment of enthalpy between the reactants and the activated complex, and the entropy of such a complex. However, the nature of the active sites is not expected to change in an oxide series, but the acid strength and distribution and the resultant "averaged-E_a" changes and observed. A plot of E_a and ln A_o for the $Cu_{1-x}Co_xFe_2O_4$ series shows a straight line (figure 9) with a very high linear regression coefficient of 0.9999 indicating the existence of a good compensation effect and hints the mechanism of PhOH ethylation remains the same at all x. Value of a and b evaluated from this plot are 10.83 and 5.80 kJ/mol respectively. ln A_o for various x values can be related to the entropy of activation of reactant species [46], and it is found that $0 < x < 0$ offers low entropy of activation than $x = 0$ or 1.

4.2. *Interaction of metal ions and electronic structure of $Cu_{1-x}Co_xFe_2O_4$ Catalysts*

XRD of spent catalysts show predominant spinel phase and a small amount of metallic Cu, α-Fe, Fe_xC_y and Cu_2O due to reductive atmosphere under ethylation conditions. This also indicates the inevitable structural collapse to some extent at $x = 0.0$; nevertheless, the structural integrity retained is high at $x \geq 0.25$ and confirmed from XRD. Further, $0 < x < 1$ compositions show almost the same and high surface Cu/Fe ratio, in spite of decreasing bulk Cu content. Contrarily, Co-content do not increase proportionately on the surface in spite of increase in bulk Co-content. Large Co-content observed at $x = 1$ shows low and decreasing catalytic activity with reaction time. All the above clearly hints that Cu^{2+} is the species that enhances the ethylation activity largely and there is a sizeable redistribution of cations on the surface during TS.

Number of changes observed in XPS from fresh to spent catalysts throws more light on the changes that are occurring under experimental conditions. A partial reduction of Cu with increasing 3d band overlap and redistributing metal ions on spent catalysts for $x < 1$. Detailed XPS analysis demonstrates the above changes are necessary from the reaction point of view. A change from low catalytic activity observed at $x = 1$ to better and desired activity found at $x \leq 0.75$ along with large Cu-species distribution on the surface demonstrate the predominant contribution of Cu^{2+} towards ethylation. Desired reaction pattern observed at $x = 0.5$ is attributed to an optimum distribution of metal ions on surface and bulk at $x = 0.5$ to have a larger 3d band overlap, in addition to the above point. These factors enhances the heterogeneity of the surface chemically and integrate the material electronically in such a way that multireactions are carried out in close proximity. This also indicates the synergism and effective utilization of reactants on ferrospinel catalyst at $0 < x < 1$. High coke content at $x = 0.75$ and low surface Co-content at $x = 0.25$ is attributed to the lower ethylation capacity compared to $x = 0.5$.

Largest yield of 2EP with high PhOH conversion and a $Cu/(Co + Fe) = 1.12$ for $x = 0.5$ insist on the optimum distribution of active species to have a highly heterogeneous surface. This also minimizes the direct interaction among same metal ions. Further, coke content increases from $x = 0.25$ to 0.75 (table 4) and decreases metal-ion concentration. Nevertheless, high $Co + Fe$ enriched surface at $x = 1$ shows poor ethylation activity and indicates the role of Fe and Co is less on ethylation. IR results [21] are concurrent with the above points and substantiate the high acidic surface does not favor the reaction.

XPS results in the present study clearly indicate that the Cu and Co 3d bands and their overlap play a central role in the catalytic performance in the ethylation reaction. Cu-rich composition ($x = 0.0$) exhibits a significant reduction of Cu species in XRD (figure 1) and it is possibly due to significantly large EtOH reforming and H_2 production. However, the addition of Co suppresses the above processes to a considerable level and utilizes H_2 for hydrogenating carbon species [47] is evident from the decrease in Cu^0-content (figure 1) and a simultaneous increase in ethylation activity from $x = 0.25$ to 0.5 compared to $x = 0$ (figure 8). The above

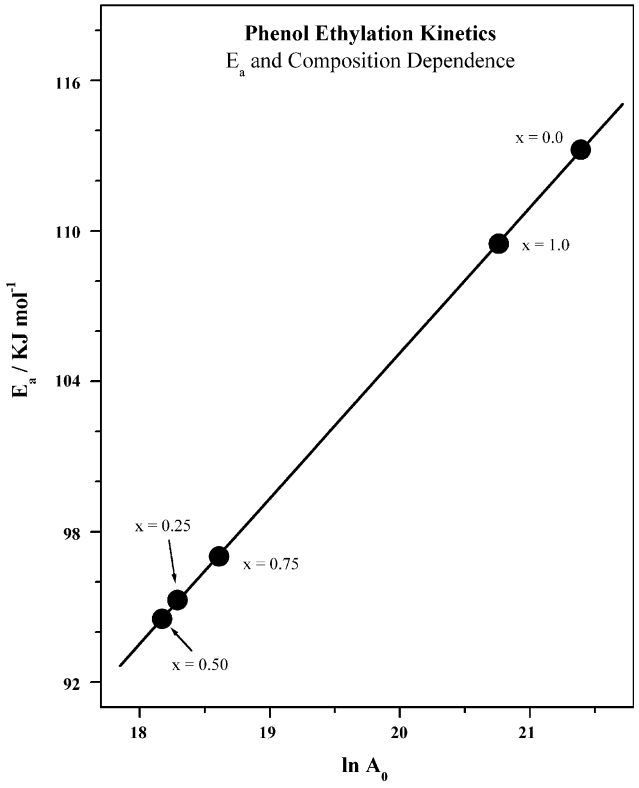

Figure 9. Activation energy is plotted against the frequency factor for $Cu_{1-x}Co_xFe_2O_4$ catalysts. Note the low activation energy with intermediate compositions compared to end compositions of catalyst.

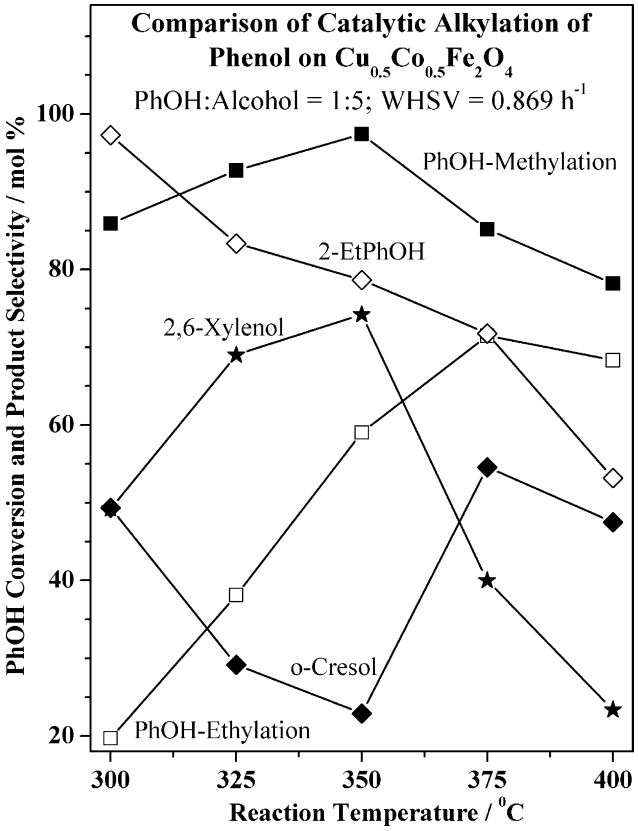

Figure 10. A comparison of catalytic activity of $Cu_{0.5}Co_{0.5}Fe_2O_4$ under identical conditions, except alkylating agent, towards ethylation and methylation of phenol between 300 °C and 400 °C, TOS = 3 h, alcohol : phenol = 5 : 1 and WHSV = 0.869 h^{-1}.

process is preferred in the presence of Co, unlike the reduction of Cu^{2+}, as in $x = 0$.

4.3. Comparison of phenol ethylation and phenol methylation

A comparison of PhOH ethylation and PhOH methylation [18–20] brings out the similarities and differences between them. Figure 10 displays a comparison of both alkylations activity under same conditions with $Cu_{0.5}Co_{0.5}Fe_2O_4$ from 300 to 400 °C. Above comparison indicates a less overall catalytic activity in ethylation than that in methylation; however, there is a same qualitative trend observed in both alkylations. A main aspect is the very high conversion of PhOH in methylation compared to ethylation. Additionally, the maximum methylation achieved at relatively low 350 °C is shifted to high 375 °C in ethylation. Another stark difference is the lack of formation of exclusive ortho ethylated products. Although ortho dimethylation is highly favored, in addition to exclusive ortho methylation, the same for diethylation is very low in addition to side products. The maximum achieved ortho diethylation selectivity is < 15% over Cu rich samples at 375 °C against 76% selectivity towards 2,6-xylenol over $x = 0.50$ at 350 °C. This indicates, the steric hindrance of alkylation species is a very important factor for efficient ortho mono and dialkylation. PhOH methylation indicates that dimethylated product is formed through sequential methylation [20]. Hence, single ortho methylated product is very much essential to reside sufficiently long time on catalyst surface for its further methylation to form ortho dimethylated product. However, the steric hindrance of ethyl group might be not favorable for proper orientation of 2EP on $Cu_{1-x}Co_xFe_2O_4$ surfaces for subsequent ortho ethylation. Besides, an intermediate acidic character observed at $x = 0.5$ correlates well with both alkylation activity and low activity at $x = 1$ indicates a highly acidic surface does not favor alkylation.

XPS studies on spent catalysts of $Cu_{1-x}Co_xFe_2O_4$ revealed the several similarities in the correlation between the catalytic performance of ethylation reaction as in methylation [20]. Both an increasing 3d bands overlap and redistribution of metal ions from fresh to spent catalysts and reducibility of Cu coincides well in the above two alkylation reactions. However, the extent of reduction occurred on spent catalysts due to ethylation is almost same between $x = 0$ and 0.5 compared to decreasing Cu-reducibility with increasing x due to methylation [20]. This clearly demonstrates that alkylating agent is mainly responsible for bringing reduction to different extent on metal ions. The role of Cu is generally

high for better alkylation activity. Spent catalyst ($x = 0.5$) shows a Cu/Co + Fe ratio of 0.89 [20] and 1.12 for methylation and ethylation respectively, suggest the heterogeneity of the catalyst surface is also important for alkylation reactions. Unlike in methylation, spent catalyst from ethylation reaction contains more Cu^{2+} and less coke species. This reflects the catalyst stability towards ethylation in maintaining high yield even after 50 h compared to the yield at TOS = 1–5 h; nonetheless, the rate of deactivation is relatively fast with methylation for the same TOS. It indicates the large utilization of EtOH compared to MeOH.

5. Conclusions

This paper reports the results from the catalytic study of PhOH ethylation on $Cu_{1-x}Co_xFe_2O_4$ ferrospinel over a wide range of temperatures and catalyst composition with a reactants composition of PhOH : EtOH of 1 : 5. Fresh and spent catalysts were subjected to detailed analysis by XRD, XPS and XAES. It has been shown that phenol ethylation leads to aromatic C-alkylation resulting in 2-EP as the major product irrespective of the reaction parameters. Cu-rich compositions display a stable activity for at least 50 h. With an increase in TOS, 2EP selectivity increases at the extent of secondary reaction products. Intermediate compositions show better activity and unique behavior than $x = 0$ and 1 emphasizing the importance of both Cu and Co for overall better performance. Coexistence of Co and Cu is also essential for minimizing side reactions by hydrogenating C species to alkyl species. Declining PhOH conversion with increasing TOS on $CoFe_2O_4$ indicates the role of Co is less in ethylation. Arrhenius plots shows relatively low E_a for $0 < x < 1$ compared to $x = 0$ and 1. An existence of the compensation effect between E_a and ln A_o has been shown, which suggests the mechanism remains the same at all x values.

XPS analysis of both fresh and spent $Cu_{1-x}Co_xFe_2O_4$ catalysts shows the oxidation states of the metal ions and its distribution on the surface have considerable influence on activity and selectivity towards phenol ethylation. During the course of the reaction, redistribution of metal ions as well as the partial reduction of metal ions to various levels occurred which ultimately determine the catalytic performance in terms of activity and stability. It is found that the heterogeneous distribution of reactive Cu species with a combination of Co and Fe is very much essential for high activity. The unique behavior of intermediate compositions towards phenol conversion is attributed to the achievement of almost same value of (Cu + Co)/Fe surface ratio during the course of the reaction. Valence band shows a change from marginal overlap between 3d bands of Cu and Co on fresh catalysts to a large overlap on spent catalysts. Cu–Co synergism observed in these materials is supported by the results from valence band, core levels and kinetic results of high catalytic performance at $x = 0.5$. In general, relatively highly acidic Co displays low catalytic activity and an intermediate acidic character that results due to a combination of Cu and Co demonstrates large catalytic activity.

Acknowledgment

TM and NRS thank CSIR, New Delhi for senior research fellowship.

References

[1] H. Fiege, *Ullmann's Encyclopedia of Industrial Chemistry; Federal Republic of Germany*, Vol. A19 (A.G. Bayer, Leverkusen) p. 324.
[2] S. Patinuin and B.S. Friedman, *Alkylation of Aromatics with Alkenes and Alkanes in Friedel Crafts and Related Reactions*,Vol. 3, ed. G.A. Olah, (Interscience, New York, 1964) p. 75.
[3] S. Sato, R. Takahashi, T. Sodesawa, K. Matsumoto and Y. Kamimura, J. Catal. 184 (1999) 180.
[4] K. Tanabe and T. Nishizaki, in: *Procceedings 6th International Congress on Catalysis*, ed. F.C. Tompkins (The Chemical Society, London, 1977).
[5] T. Kotanigawa, M. Yamamoto, K. Shimokawa and Y. Yoshida, Bull. Chem. Jpn. 44 (1971) 1961.
[6] M. Inoue and S. Emoto, Chem. Pharm. Bull. 20 (1972) 232.
[7] H. Saltonstall and A. Settle, J. Am. Chem. Soc. 71 (1949) 943.
[8] R. Stroh, R. Seydel and W. Hahn, in: *Neuere Methoden der praparatively organischen chemie* , ed. W. Foerst (Verlag-Chemie, Weinheim 2, 1960) p. 231.
[9] Z.P. Aleksandrova, J. Gen. Chem. (U.S.S.R). 12 (1942) 522.
[10] A.G. Bayer, EP 102 493, 1983.
[11] S. Velu and C.S. Swamy, Res. Chem. Intermed. 26 (2000) 295.
[12] K. Sreekumar, T. Mathew, R. Rajagopal, R. Vetrivel and B.S. Rao, Catal. Lett. 65 (2000) 99.
[13] K. Sreekumar, T. Mathew, S.P.Mirajkar, S. Sugunan and B.S. Rao, Appl. Catal. A 201 (2000) L1.
[14] K. Sreekumar, T. Mathew, B.M. Devassy, R. Rajagopal, R. Vetrivel and B.S. Rao, Appl. Catal. A 205 (2001) 11.
[15] K. Sreekumar, T.M. Jyothi, T. Mathew, M.B. Talawar, S. Sugunan and B.S. Rao, J. Mol. Catal. A 159 (2000) 327.
[16] B.S. Rao, K. Sreekumar and T.M. Jyothi, Indian Patent 2707/98 (1998).
[17] P.S. Anilkumar, J.J. Shrotri, S.D. Kulkarni, C.E. Deshpande and S.K. Date, Mater. Lett. 27 (1996) 293.
[18] T. Mathew, Ph.D Thesis, Synthesis and characterization of mixed oxides containing cobalt, copper and iron and study of their catalytic activity, University of Pune, 2002.
[19] K. Lázár, T. Mathew, Z. Koppány, J. Megyeri, V. Samuel, S.P. Mirajkar, B.S. Rao and L. Guczi, Phys. Chem. Chem. Phys. 4 (2002) 3530.
[20] T. Mathew, N.R. Shiju, K. Sreekumar, B.S. Rao and C.S. Gopinath, J. Catal. 210 (2002) 405; T. Mathew, B.S. Rao and C.S. Gopinath, J. Catal. 222 (2004) 107; and references therein.
[21] T. Mathew, N.R. Shiju, B.B. Tope, S.G. Hegde, B.S. Rao and C.S. Gopinath, Phys. Chem. Chem. Phys. 4 (2002) 4260.
[22] M.K. Dongare, V. Ramaswamy, C.S. Gopinath, A.V. Ramaswamy, S. Scheurell, M. Brueckner and E. Kemnitz, J. Catal. 199 (2001) 209.
[23] V.L.J. Joly, P.A. Joy, S.K. Date and C.S. Gopinath, J. Phys. Cond. Matt. 13 (2001) 649.
[24] G. Moretti, G. Fierro, M.L. Jacono and P. Porta, Surf. Interface Anal. 14 (1989) 325.

[25] S. Poulston, P.M. Parlett, P. Stone and M. Bowker, Surf. Interface Anal. 24 (1996) 811.
[26] B.R. Strohmeier, B.E. Leyden, R.S. Field and D.M. Hercules, J. Catal. 94 (1985) 514.
[27] J.H. Scofield, J. Electron Spectrosc. Relat. Phenom. 8 (1976) 129.
[28] T. Yamaguchi, Proc. Fac. Eng. Keiogijuku Univ. 19 (1967) 776.
[29] G. van der Laan, C. Westra, C. Haas and G.A. Sawatzky, Phys. Rev. B 23 (1981) 4369.
[30] M.S. Stranick, M. Houalla and D.M. Hercules, J. Catal. 106 (1987) 362.
[31] N.S. McIntyre and M.G. Cook, Anal. Chem. 47 (1975) 2210.
[32] Z. Zsoldos and L. Guczi, J. Phys. Chem. 96 (1992) 9393.
[33] P. Mills and J.L. Sullivan, J. Phys. D16 (1983) 723.
[34] T. Fujii, F.M.F. de Groot, G.A. Sawatzky, F.C. Voogt, T. Hibma and K.Okada, PRB 59 (1999) 3195.
[35] J.J. Yeh, I. Lindau and At. Data Nucl. Data Tables 32 (1985) 1.
[36] S. Velu, K. Suzuki, C.S. Gopinath, H. Yoshida and T. Hattori, PCCP 4 (2002) 1990.
[37] S. Velu, K. Suzuki and C.S. Gopinath, J. Phys. Chem. B 106 (2002) 12737.
[38] K. Li, I. Wang and K. Chang, Ind. Eng. Chem. Res. 32 (1993) 1007.
[39] F.M. Bautista, J.M. Campelo, A. Garcia, D. Luna, J.M. Marinas, A. Romero, J.A. Navio and M. Macias, Appl. Catal. 99 (1993) 161.
[40] E. Santacesaria, M. Diserio, P. Ciambelli, D. Gelosa and S. Carra, Appl. Catal. 64 (1990) 101.
[41] S. Velu and C.S. Swamy, Appl. Catal. A 145 (1996) 225.
[42] P.L. Yue and O. Olaofe, Chem. Eng. Res. Des. 62 (1984) 167.
[43] F.M. Bautista, J.M. Campelo, A. Garcia, D. Luna and J.M. Marinas, J. Catal. 107 (1987) 181.
[44] A. Corma, F. Llopis, J.B. Monton and S. Weller, J. Catal. 142 (1993) 97.
[45] G.C. Bond, Catal. Rev. Sci. Engn. 42 (2000) 323.
[46] A.B. Hart and R.A. Ross, J. Catal. 2 (1963) 121 and 251.
[47] G. Fornasari, A.D. Huysser, L. Mintcher, F. Trifiro and A. Vaccari, J. Catal. 135 (1992) 386.